CHEMICAL ENGINEERING TRANSACTIONS
VOL. 74, 2019
A publication of AIDIC
The Italian Association of Chemical Engineering
Online at www.cetjournal.it
Guest Editors: Sauro Pierucci, Jiří Jaromír Klemeš, Laura Piazza
Copyright © 2019, AIDIC Servizi S.r.l.
ISBN 978-88-95608-71-6; **ISSN** 2283-9216
DOI: 10.3303/CET1974008

Syngas Production through H_2O/CO_2 Thermochemical Splitting

Maria Portarapillo[a], Antonio Aronne[a], Almerinda Di Benedetto[a], Claudio Imparato[a], Gianluca Landi[b*], Giuseppina Luciani[a]

[a]Dipartimento di Ingegneria Chimica, dei Materiali e della Produzione Industriale, Università di Napoli Federico II, Naples, Italy
[b]Institute of Research on Combustion – CNR, Naples, Italy
gianluca.landi@cnr.it

CO_2 and H_2O can be energy-upgraded through solar thermochemical cycles. Suitable redox materials are reduced in a solar reactor at high temperature (above 1300-1400°C) and afterwards re-oxidised by CO_2 and/or H_2O flow, thus producing CO and/or H_2. Ceria was recognised as one of the most interesting materials for this process. However, high reduction temperature, low re-oxidation kinetics as well as low stability hindered its practical application. In this work, the redox properties of $Ce_{0.75}Zr_{0.25}O_2$ system prepared by hydrothermal synthesis were compared with those of a co-precipitated sample with the same nominal composition used as reference. Samples were characterised by XRD and N_2 physisorption; their self-reducibility and CO_2 splitting activity were tested in a thermogravimetric balance, while H_2O splitting properties were studied in an *ad hoc* fixed bed reactor on H_2 pre-reduced samples. Obtained results proved that the material prepared by hydrothermal synthesis is characterised by both improved reducibility and splitting activity.

1. Introduction

Catalytic thermochemical cycles have received a renewed interest as a first step to produce fuels (McDaniel, 2017). In a typical cycle, a redox material is reduced at high temperature in a solar reactor and then oxidised by carbon dioxide and/or water, producing carbon monoxide and/or hydrogen.
Catalytic two-step cycles are generally preferred to multistep processes (see, for instance, Kalyva et al., 2015; Shazed et al., 2017) due to their higher theoretical efficiency and lower complexity (Rao and Dey, 2015).
Volatile and melting oxides are not used due to several issues related to the required fast quenching of gaseous products for volatile oxides, as well as crushing and sieving operations for melting oxides (Agrafiotis et al., 2015; Fu et al., 2016; Sheffe and Steinfeld, 2014).
Non-stoichiometric oxides, such as cerium dioxide and perovskites, are promising for their high structure stability during the whole cycle, even if the released oxygen quantities are lower.
Ceria is considered as the benchmark material for high temperature splitting cycles (Ruan et al., 2017). However, ceria-based cycle is characterised by low solar to fuel efficiency and thermal stability loss. Modifying the reactor/catalyst configuration (Ackermann et al., 2017; Gladen and Davidson, 2016; Tou et al., 2017) and/or prompting catalyst self-reduction by using a reducing gas in the solar reactor can improve redox performance (Nair and Abanades, 2016; Zhao Z. et al., 2016). Noteworthy, doping is the main route used to improve the CeO_2 redox properties (Bhosale et al., 2016a; Muhich and Steinfeld, 2017; Zhao B. et al., 2016), thanks to the introduction of defects. It has been shown that Ce partial substitution with zirconium can enhance splitting properties of ceria thanks to the increased oxygen diffusion in the lattice (Muhich and Steinfeld, 2017). The highest H_2 production through water splitting was shown by CeO_2-ZrO_2 systems with Ce/Zr molar ratio = 3 (Le Gal et al., 2013). Notably, the co-presence of different sites/phases has been recognized as a key feature to achieve both good catalyst self-reduction at lower temperature and good activity towards splitting reactions (Miller et al., 2014; Pappacena et al., 2016; Pappacena et al., 2017).

Paper Received: 19 May 2018; Revised: 19 November 2018; Accepted: 6 March 2019

Please cite this article as: Portarapillo M., Aronne A., Di Benedetto A., Imparato C., Landi G., Luciani G., 2019, Syngas Production Through H2o/co2 Thermochemical Splitting, Chemical Engineering Transactions, 74, 43-48 DOI:10.3303/CET1974008

Indeed, the synthesis strategy can strongly affect the final structural, morphological and redox properties of oxides and, consequently, H_2 release rate and productivity (Nair and Abanades, 2016). Among the available synthetic routes for CeO_2-ZrO_2 systems, hydrothermal synthesis ensures low cost and mild experimental conditions, providing good control on final composition as well as morphologies and structure of the nanomaterials (Papari et al., 2017).
With the aim to get insight into the effects of the synthesis method on structural/compositional features and redox performances, in this study, $Ce_{0.75}Zr_{0.25}O_2$ materials were prepared by both co-precipitation and hydrothermal synthesis. The activity of these materials towards both CO_2 and H_2O splitting were tested by thermogravimetric analysis (TGA) and flow reactor tests, respectively. Samples prepared by hydrothermal route showed higher redox performance and improved stability, providing higher CO and H_2 production than the co-precipitated sample.

2. Materials and methods

2.1 Materials preparation

Ceria-zirconia materials were prepared through co-precipitation and hydrothermal routes. All reagents were purchased from Sigma-Aldrich and used as received. Cerium (III) nitrate hexahydrate, zirconium (IV) nitrate hydrate, zirconium (IV) propoxide (70 wt% in 1-propanol), acetylacetone, anhydrous 1-propanol were employed. According to previous results (Le Gal and Abanades, 2012), Ce/Zr molar ratio was kept constant equal to 3.
The co-precipitated sample was prepared starting from an aqueous solution containing stoichiometric amounts of cerium and zirconium nitrates in 75 ml bi-distilled water and stirred for 3 h. A homogeneous gel was then obtained by heating in a MW oven (CEM SAM-155), that was further calcined at 1100°C for 4h. The so-obtained sample was labelled CZ-CP.
In the hydrothermal synthesis, a solution of cerium nitrate 0.46 M in 1-propanol dropwise added to a solution of zirconium propoxide 0.41 M in 1-propanol giving a volumetric ratio 3:1 was prepared. Then an appropriate amount of acetylacetone to obtain a molar ratio acetylacetone : zirconium (IV) propoxide = 0.5 was added. Acetylacetone is a chelating ligand commonly used to stabilise zirconium alkoxide sols in sol-gel routes, but less employed in hydrothermal processing. After two days under magnetic stirring the solution was poured into a Teflon vessel and submitted to hydrothermal treatment at 120°C overnight. After the hydrothermal treatment, the sample was centrifuged and repeatedly washed with distilled water (3 times) to remove any unreacted species, and then dried at 80°C overnight. Finally, particles were treated at 500°C in nitrogen flow for 5 h to eliminate the nitrates and adsorbed organic substances. The so-obtained sample was labelled CZ-HTA.

2.2 Materials characterization

ICP-MS analysis performed on an Agilent 7500CE instrument was used to investigate the actual composition of the materials. Results showed differences with the nominal content within the experimental error (±5%).
A XRD diffractometer PANalytical X'Pert Pro was used to collect X-ray diffraction spectra. Step size was set at 0.02° and counting time was set at 80 s per step. Average crystal size (τ) was evaluated through the Scherrer formula:

$$\tau = \frac{K \cdot \lambda}{\beta \cdot cos\theta} \quad (1)$$

where: τ is the mean size of the crystallite domains, K is a dimensionless shape factor, with value close to unity, λ is the X-ray wavelength, β is the broadening at half the maximum intensity (FWHM), θ is the Bragg angle (in radiant). A Quantachrome Autosorb-1C instrument was used to measure BET surface areas (SSA) of fresh and used materials by N_2 adsorption at 77 K; samples were degassed at 150°C for 1.5 h before the measurement.

2.3 TG analysis

TGA/DSC TA Instrument Q600SDT was used to perform TG analysis, following a previously described procedure (Luciani et al., 2018). Briefly, a 30 mg sample was placed in an alumina crucible, pre-treated in air at 1200°C (heating rate: 20°C/min) in order to remove the chemisorbed CO_2 and then cooled down to room temperature. After 1 h purging under a nitrogen flow, the sample was heated up to 1350°C (heating rate: 20°C/min) under a nitrogen flow (0.1 l(STP)/min) and kept for 50 min at 1350°C. Then it was cooled down to 1100°C and the atmosphere was switched to CO_2, followed by a first isothermal step at 1100°C for 50 min (oxidation step) and by a second isothermal step at 1000°C for 50 min.

2.4 H_2O splitting tests

The experimental rig and the experimental details were previously described (Luciani et al., 2018). Briefly, a tubular quartz reactor inserted into an electric tubular furnace (Lenton) was used to hold the powdered samples (500 mg; 170-300 µm). Temperature was monitored by means of a thermocouple placed inside the reactor. The maximum temperature achievable by the tubular furnace was about 1100°C; thus, samples were reduced by a hydrogen pre-treatment (10 l(STP)/h; 5 vol.% H_2/N_2) at about 1000°C (heating rate: 10°C/min) (Pappacena et al., 2016; Pappacena et al., 2017; Al-Shankiti et al., 2013). After cooling down to about 100°C, splitting tests were carried out by flowing a 3 vol.% H_2O/N_2 mixture (10 l(STP)/h); the temperature was raised up to about 1000°C (heating rate: 10°C/min; time at the maximum temperature: 20 min).

3. Results

3.1 Materials characterization

XRD spectra of the studied samples are shown in Figure 1. Each profile shows main peaks at 2θ = 28.870°, 48.049°, 57.012°, assigned to (1,1,1), (2,2,0) and (3,1,1) planes in a fluorite structure, typical of the CeO_2-ZrO_2 system. CZ-CP shows more intense and defined peaks, thus indicating a larger crystalline size than CZ-HTA (Table 1) as a consequence of the higher calcination temperature used for the co-precipitated sample. Actually, the hydrothermal synthesis is expected to allow small crystal size and high surface area. XRD carried out on samples after TG analysis (not reported) do not show significant qualitative differences, thus excluding de-mixing phenomena.
BET analysis has been carried out on the samples as prepared and after a redox cycle in TG; results are given in Table 1. CZ-HTA sample shows a higher surface area than the co-precipitated sample, both before and after TG tests. However, SSA of the CZ-HTA sample decreases after one redox cycle, likely because of sintering induced by the high temperature reached. On the contrary, specific surface areas of the CZ-CP sample before and after the redox cycle are very similar.

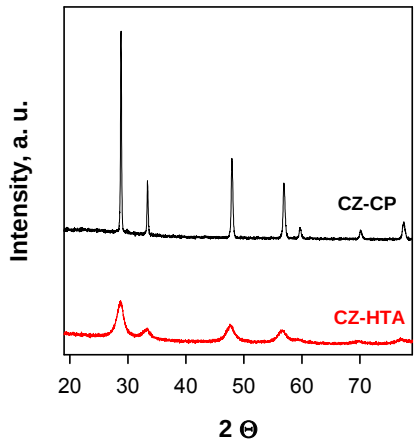

Figure 1: XRD profiles of the studied samples.

Table 1: Average crystallite size and specific surface areas of the samples

Sample	τ, nm	SSA, m^2/g	SSA*, m^2/g
CZ-CP	23.9	3	4
CZ-HTA	3.6	112	12
*after redox tests in TG			

3.2 TG analysis

Air pre-treatment in air up to 1200°C was performed in situ in order to remove any carbonate species formed during samples storage and handling.
In Figure 2, the TG profiles of both samples during a red-ox cycle are shown. Due to air pre-treatment, mass losses in TG curve during heating under nitrogen flow are directly related to O_2 evolution. In particular, the weight loss of the CZ-CP sample starts at about 1100°C, whereas the CZ-HTA is easily reducible, since its reduction starts at 1000°C. Moreover, TG curve of CZ-HTA features a higher slope, thus suggesting faster

reduction kinetics than CZ-CP sample. Finally, the sample prepared by hydrothermal synthesis is also more reducible, as pointed out by the larger weight loss.
As reported in Figure 2, reduced samples were re-oxidised by exposing them to CO_2 after cooling down to 1100°C and 1000°C; the corresponding weight rises are due to re-oxidation and simultaneous CO evolution. Temperature poorly affects weight gains independently from the preparation method during the oxidation steps. On the contrary, isothermal cycles at 1350°C are characterised by very low CO production (not reported). Thus, the oxidation temperature, which depends on several factors (Ehrhart et al., 2016), should be chosen in order to obtain the highest solar-to-fuel efficiency of the cycle. The CZ-HTA sample shows the highest weight regain. Accordingly, hydrothermal synthesis allowed to improve both self-reducibility and CO_2 splitting properties.
From the quantitative point of view, O_2 productions on CZ-CP and CZ-HTA were about 220 and 470 µmol/g respectively, while CO productions were about 63 and 80 µmol/g, respectively. The performance of CZ-HTA sample agrees with the literature results (Bhosale et al., 2016b; Zhao B. et al., 2016).

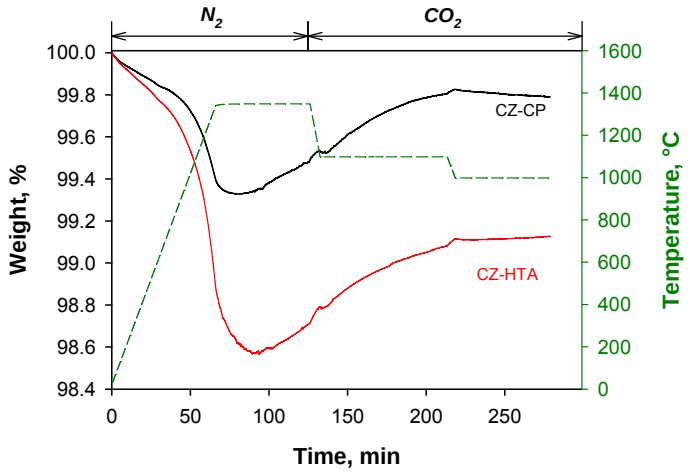

Figure 2: TG profiles of a CO_2 splitting cycle on the studied samples.

3.3 H_2O splitting tests

Reduction profiles (not reported) show one or two unresolved peaks at low temperature (400-600°C) and a high temperature peak (T ≥ 800°C), that can be associated to surface and bulk reduction respectively (Trovarelli, 2002). H_2 evolution profiles (not reported) during H_2O splitting tests are simpler and characterised by one or two well-defined peaks. CZ-CP showed a single oxidation peak at about 350-400°C, while CZ-HTA is oxidised showing two peaks at 250°C and 600°C, with the former larger than the latter.
From the quantitative point of view (Figure 3), it is worth noting that higher reduction degree was obtained by hydrogen pre-treatment with respect to self-reduction under nitrogen (i.e. during TGA). CZ-CP showed the lowest amount of released oxygen and produced hydrogen as well as incomplete re-oxidation (about 50%). On the contrary, CZ-HTA produced more hydrogen than expected during the first cycle and showed a high re-oxidation degree (about 90%) during the second cycle. Surprisingly, samples showed similar reduction degrees during the first cycle, while re-oxidations were different, CZ-HTA showing the larger H_2 production. This suggests that the sample prepared by hydrothermal synthesis is characterised by a faster oxidation kinetics, as confirmed by oxidation behaviour observed during H_2O splitting tests.
Interestingly, the CZ-HTA sample showed negative reduction degree at the end of the first oxidation step; a significant Ce^{3+} fraction in this sample could explain this behaviour. It is worth noting that thermochemical splitting reactions (i.e. reduction and oxidation) involve both surface reactivity and bulk redox properties, linked through oxygen diffusion from the bulk to the surface (during reduction) and *vice versa* (during oxidation). It could be inferred that Ce^{3+} ions in the CZ-HTA sample are (not homogeneously) distributed both at surface and in the bulk phase. According to previous findings, oxygen vacancies (related to Ce^{3+} ions) at the surface are active sites for water dissociation (OH groups on the surface are obtained) (Clarizia et al., 2017), while the corresponding Ce^{3+} sites promote H_2 formation by weakening H-O bonds (Pappacena et al., 2017). Moreover, oxygen defects in the bulk phase (related to the bulk Ce^{3+} fraction) promote oxygen diffusion between the surface and the bulk, thus leading to a faster re-formation of surface oxygen vacancies (Pappacena et al., 2017). The relationship between redox properties and Ce^{3+} fraction on CZ-CP and CZ-HTA samples is under investigation.

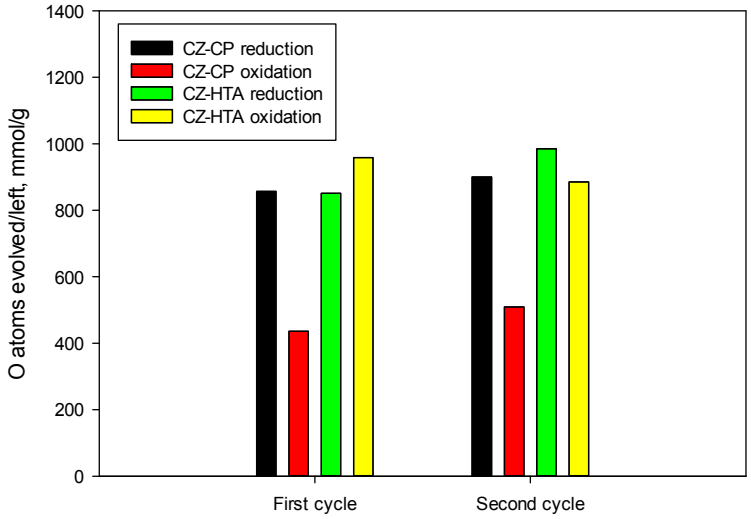

Figure 3: Amount of oxygen atoms released during H_2 pre-treatment and gained the materials during H_2O splitting tests for different cycles.

4. Conclusions

In this work the effect of the preparation method on the splitting performance of $Ce_{0.75}Zr_{0.25}O_2$ system was investigated. The redox properties of a sample prepared by hydrothermal synthesis were compared to those of a co-precipitated ceria-zirconia sample, used as a reference.
The material prepared by hydrothermal method showed lower crystallite size, as expected, as well as larger specific surface area both before and after high temperature redox cycles.
Results of splitting tests on CO_2 and H_2O agreed that the material prepared by hydrothermal synthesis is characterized by both improved reducibility and splitting activity.
A possible explanation of this behaviour could be related to a higher bulk and surface Ce^{3+} fraction in the material prepared by hydrothermal route. As a matter of fact, Ce^{3+} ions are directly related to oxygen vacancies, which are the active sites for CO_2/H_2O activation on the surface and improve the oxygen diffusivity in the bulk phase.

Acknowledgments

The authors gratefully acknowledge Mr. Andrea Bizzarro for BET analysis and Mr. Fernando Stanzione for ICP-MS measurements.

References

Ackermann S., Takacs M., Scheffe J., Steinfeld A., 2017, Reticulated porous ceria undergoing thermochemical reduction with high-flux irradiation, Int. J. Heat Mass Transf., 107, 439–449.
Agrafiotis C., Roeb M., Sattler C., 2015, A review on solar thermal syngas production via redox pair-based water/carbon dioxide splitting thermochemical cycles, Renew. Sustain. Energy Rev., 42, 254–285.
Al-Shankiti I., Al-Otaibi F., Al-Salik Y., Idriss H., 2013, Solar Thermal Hydrogen Production from Water over Modified CeO2 Materials, Top. Catal., 56, 1129–1138.
Bhosale R.R., Kumar A., Almomani F., Ghosh U., Al-Muhtaseb S., Gupta R., Alxneit I., 2016a, Assessment of CexZryHfzO2 based oxides as potential solar thermochemical CO2 splitting materials, Ceram. Int., 42, 9354–9362.
Bhosale R.R., Kumar A., AlMomani F., Alxneit I., 2016b, Sol-gel derived CeO2-Fe2O3 nanoparticles: Synthesis, characterization and solar thermochemical application, Ceram. Int., 42, 6728–6737.
Clarizia L., Vitiello G., Pallotti D.K., Silvestri B., Nadagouda M., Lettieri S., Luciani G., Andreozzi R., Maddalena P., Marotta R., 2017, Effect of surface properties of copper-modified commercial titanium dioxide photocatalysts on hydrogen production through photoreforming of alcohols, Int. J. Hydrogen Energy., 42, 28349–28362

Ehrhart B.D., Muhich C.L., Al-Shankiti I., Weimer A.W., 2016, System efficiency for two-step metal oxide solar thermochemical hydrogen production – Part 1: Thermodynamic model and impact of oxidation kinetics, Int. J. Hydrogen Energy, 41, 19881–19893

Fu Y., Li S., Zhang J., Sun Y., 2016, Effective Macroporous Core-Shell Structure of Alumina-Supported Spinel Ferrite for Carbon Dioxide Splitting Based on Chemical Looping, Energy Technol., 4, 1349–1357.

Gladen A.C., Davidson J.H., 2016, The morphological stability and fuel production of commercial fibrous ceria particles for solar thermochemical redox cycling, Sol. Energy., 139, 524–532.

Kalyva A.E., Vagia E.Ch., Konstandopoulos A.G., Srinivasa A.R., T-Raissi A., Muradov N., Kakosimos K.E., 2015, Investigation of the solar hybrid photo-thermochemical sulfur-ammonia water splitting cycle for hydrogen production, Chem. Eng. Trans., 45, 361–366.

Le Gal A., Abanades S., 2012, Dopant incorporation in ceria for enhanced water-splitting activity during solar thermochemical hydrogen generation, J. Phys. Chem. C, 116, 13516–13523

Le Gal A., Abanades S., Bion N., Le Mercier T., Harlé V., 2013, Reactivity of doped ceria-based mixed oxides for solar thermochemical hydrogen generation via two-step water-splitting cycles, Energy and Fuels., 27, 6068–6078.

McDaniel A.H., 2017, Renewable energy carriers derived from concentrating solar power and nonstoichiometric oxides, Curr. Opin. Green Sustain. Chem., 4, 37–43.

Miller J.E., McDaniel A.H., Allendorf M.D., 2014, Considerations in the Design of Materials for Solar-Driven Fuel Production Using Metal-Oxide Thermochemical Cycles, Adv. Energy Mater., 4, 1300469.

Muhich C., Steinfeld A., 2017, Principles of doping ceria for the solar thermochemical redox splitting of H2O and CO2, J. Mater. Chem. A, 5, 15578–15590.

Nair M.M., Abanades S., 2016, Tailoring Hybrid Nonstoichiometric Ceria Redox Cycle for Combined Solar Methane Reforming and Thermochemical Conversion of H2O/CO2, Energy and Fuels., 30, 6050–6058.

Papari G.P., Silvestri B., Vitiello G., De Stefano L., Rea I., Luciani G., Aronne A., Andreone A., 2017, Morphological, Structural, and Charge Transfer Properties of F-Doped ZnO: A Spectroscopic Investigation, J. Phys. Chem. C, 121, 16012–16020.

Pappacena A., Boaro M., Armelao L., Llorca J, Trovarelli A., 2016, Water splitting reaction on Ce0.15Zr0.85O2 driven by surface heterogeneity, Catal. Sci. Technol., 6, 1–9.

Pappacena A., Rancan M., Armelao L., Llorca J., Ge W., Ye B., Lucotti A., Trovarelli A., Boaro M., 2017, New Insights into the Dynamics That Control the Activity of Ceria-Zirconia Solid Solutions in Thermochemical Water Splitting Cycles, J. Phys. Chem. C., 121, 17746–17755.

Rao C.N.R., Dey S., 2015, Generation of H2 and CO by solar thermochemical splitting of H2O and CO2 by employing metal oxides, J. Solid State Chem., 242, 107–115.

Ruan C., Tan Y., Li L., Wang J., Liu X., Wang X., 2017, A novel CeO2-xSnO2/Ce2Sn2O7 pyrochlore cycle for enhanced solar thermochemical water splitting, AIChE J., 63, 3450–3462.

Shazed A.R., Kalyva A.E., Vagia E.C., Srinivasa A.R., Traissi A., Muradov N., Kakosimos K.E., 2017, Chemical plant analysis of hydrogen production based on the hybrid sulfur-ammonia water splitting cycle, Chem. Eng. Trans., 61, 433–438.

Scheffe J.R., Steinfeld A.,2014, Oxygen exchange materials for solar thermochemical splitting of H2O and CO2: A review, Mater. Today., 17, 341–348.

Trovarelli A., 2002, Catalysis by Ceria and Related Materials, Imperial College Press

Tou M., Michalsky R., Steinfeld A., 2017, Solar-Driven Thermochemical Splitting of CO2 and In Situ Separation of CO and O2 across a Ceria Redox Membrane Reactor, Joule., 1, 146–154.

Zhao B., Huang C., Ran R., Wu X., Weng D., 2016, Two-step thermochemical looping using modified ceria-based materials for splitting CO2, J. Mater. Sci., 51, 2299–2306.

Zhao Z., Uddi M., Tsvetkov N., Yildiz B., Ghoniem A.F., 2016, Redox Kinetics Study of Fuel Reduced Ceria for Chemical-Looping Water Splitting, J. Phys. Chem. C., 120, 16271–16289.